REVIEW OF NUMERICAL SIMULATION OF MIXING DUE TO RAYLEIGH-TAYLOR AND RICHTMYER-MESHKOV INSTABILITIES

David Youngs

AWE

Aldermaston

UK

Scope: 2D and 3D numerical simulation (DNS or LES) of the non-linear growth of Rayleigh-Taylor and Richtmyer-Meshkov instabilities.

Reasons for numerical simulation

(a) gain understanding of the mixing processes which is not available from experiment

(b) explain experimental results

(c) design experiments

(d) provide results for the calibration of engineering models (eg RANS models)

(e) full simulation of engineering applications

(a) **2D single mode**

(b) 2D multimode

(c) Additional physics

(d) 3D single mode/few modes

(e) 3D turbulence
modelling of the unresolved scales

(f) Future role of numerical simulation
AWE examples

Aim to illustrate the progress made with examples – not a complete review of all the work done.

Turbulent mixing is a 3D process.

However, the dynamics of the large scale structures within the mixing layer is the key aspect of mixing and much has been/can still be learnt about this from single-mode or 2D multimode simulations.

The fine-scale structure (dissipation at high wave numbers) is essentially a 3D process and for this 3D simulation is essential.

The possibilities of 3D simulation on present-day super computers should be fully exploited – however, simpler 2D simulation still has an essential role especially for complex problems with additional physics.

2D SINGLE MODE

The first 2D simulations of RT were carried out in Frank Harlow's group at LANL in the late 1960s.

e.g. B J Daly, Phys Fluids Vol 10, p297 (1967)

MAC code: **incompressible**
'Marker and Cell'

$\frac{\rho_1}{\rho_2} = 1.1, 2, 10$

Roll-up of the spike due to Kelvin-Helmholtz instability seen for

$\frac{\rho_1}{\rho_2} = 1.1, \text{and } 2,$ **but not for** $\frac{\rho_1}{\rho_2} = 10.$

not observed experimentally until Ratafia, Phys Fluids Vol 16 p1207 (1973).

results explained by drag force on bubble and spike – as in buoyancy – drag models which are widely used today.

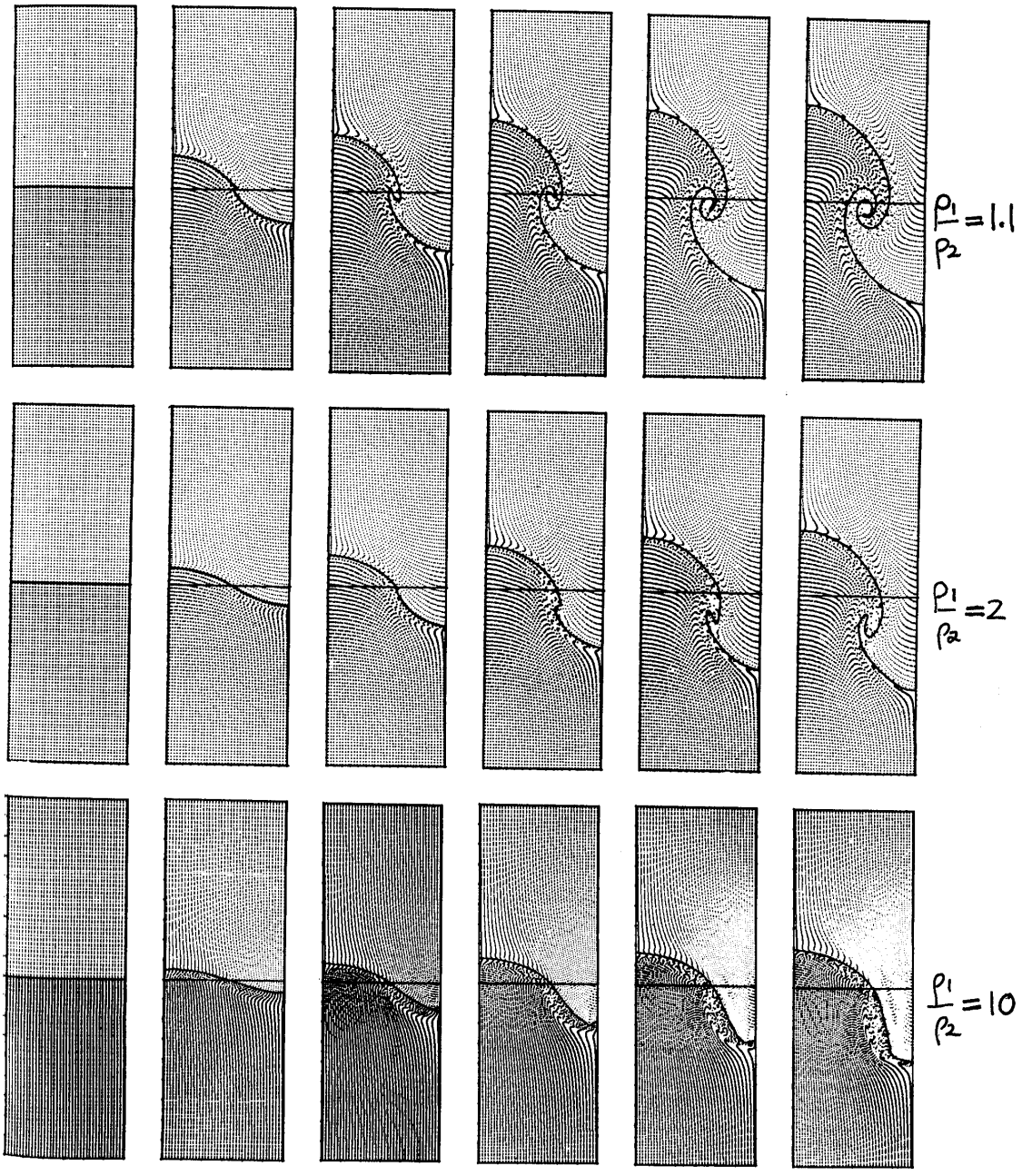

Physics of Fluids, vol 10, p297 (1967)

Youngs, Physica 12D, p32 (1984)

2D Eulerian code

- **Interface tracking (VOF technique)**
- **Monotonic advection method of Van Leer for all fluid variables**

  $\Rightarrow$ **improved numerical stability over the earlier hydrocodes**

Shows KH instability on the spike at high density ratio, $\frac{\rho_1}{\rho_2} = 20$

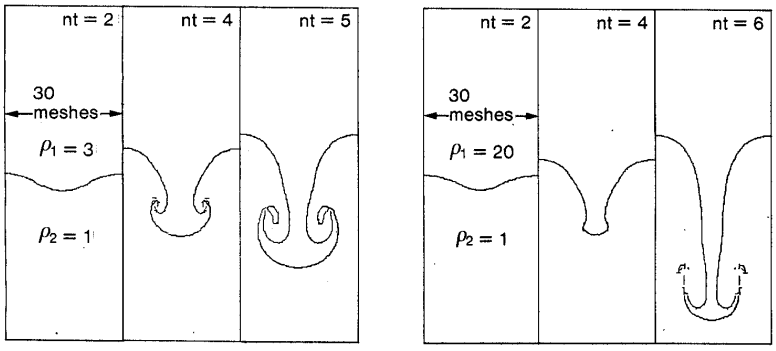

Fig. 1. Rayleigh–Taylor instability, single wavelength initial perturbation.

Youngs, Physica 12D, p19 (1984)

2D Multimode Rayleigh-Taylor triggered by short wavelength random perturbations. Incompressible hydrocode similar to MAC code but interface tracking was abandoned as fine-scale mixing expected.

Solved equation for fluid 1 volume fraction

$$\frac{\partial f_1}{\partial t} + \mathrm{div}\left(f_1 \underline{u}\right) = 0$$

Showed self-similar growth with bubble penetration (h_1) given by

$$h_1 = \alpha \frac{\rho_1 - \rho_2}{\rho_1 + \rho_2} g t^2$$

$\alpha \approx$ **0.04 to 0.05 independent of density ratio, for growth by mode coupling.**

Subsequent experiments, Read, Physica 12D, p45 (1984) gave $\alpha \sim$ **0.06 to 0.07.**

At the time difference between α **in calculation and experiment was attributed to 2D vs 3D effects – but this has not turned out to be so simple.**

I-L Chern, J Glimm et al
J Comp Phys, vol 62, p64 (1986)

Fron Tier: **Accurate front tracking technique (more accurate than the VOF techniques)**

Applied to multimode 2D RT in Glimm et al Phys Fluids A2 p2046 (1990)

Note that most of RT experiments use immiscible liquids – so need to eliminate mass diffusion.

Results used to develop bubble merger models.

For two generations of bubble merger simulations give $\alpha \sim 0.055$ to 0.065 in agreement with experiment.

For more than two generations α drops to ~ 0.04 (fine-scale structure develops).

Glimm et al (1990)

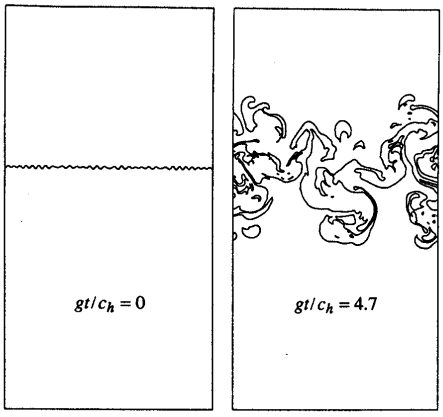

FIG. 10. Plots of interfaces in the random disturbance simulation of Rayleigh–Taylor instability. The Atwood number is $A = \frac{1}{3}$ and the compressibility is $M^2 = 0.1$. The acceleration rate of the bubble envelope has good agreement with the experiment of Read for $1\frac{1}{2}$ generations of bubble merger. The acceleration rate decreases after this time because of the multiphase connectivity, which is different in the exactly two-dimensional computation and in the approximately two-dimensional experiments.

Inogamov (3rd IWPCTM) argued that self similar gt^2 growth should be obtained if a multimode perturbation with

$$\frac{\text{amplitude}}{\text{wavelength}} = \varepsilon \text{ (a constant)}$$

is used. In this case α depends weakly on the initial conditions.

2D multimode calculations described by Atzeni and Guerrieri, Europhys Lett, Vol 22, p603 (1993).

α ~ 0.04 to 0.05 lower bound for mix evolution.

Demonstrates the very useful role which numerical simulation can play in understanding the effect of initial conditions on turbulent mixing.

What happens in real problems?

Growth via mode coupling

or growth directly from initial perturbations.

RICHTMYER-MESHKOV: 2D SINGLE MODE

Impulsive linear model (Richtmyer)

$$\frac{da}{dt} = \frac{2\pi}{\lambda} A^+ a_o^+ \Delta U$$

A^+, a_o^+: **post shock Atwood Number and amplitude**

2D numerical simulation very useful in understanding the correct effect of compressibility on the linear theory and also the non-linear behaviour.

Highlight recent paper:-

Holmes, Dimonte, Fryxell, Gittings, Grove, Schneider, Sharp, Velikovich, Weaver, Zhang. J Fluid Mech, Vol 389, p55 (1999)

Compare three different hydrocodes (RAGE, PROMETHEUS and Fron Tier) with non-linear theory, and with a NOVA experiment.

Fron Tier:	**interface tracking**
RAGE:	**no interface tracking, AMR**
PROMETHEUS:	**no interface tracking (MUSCL)**

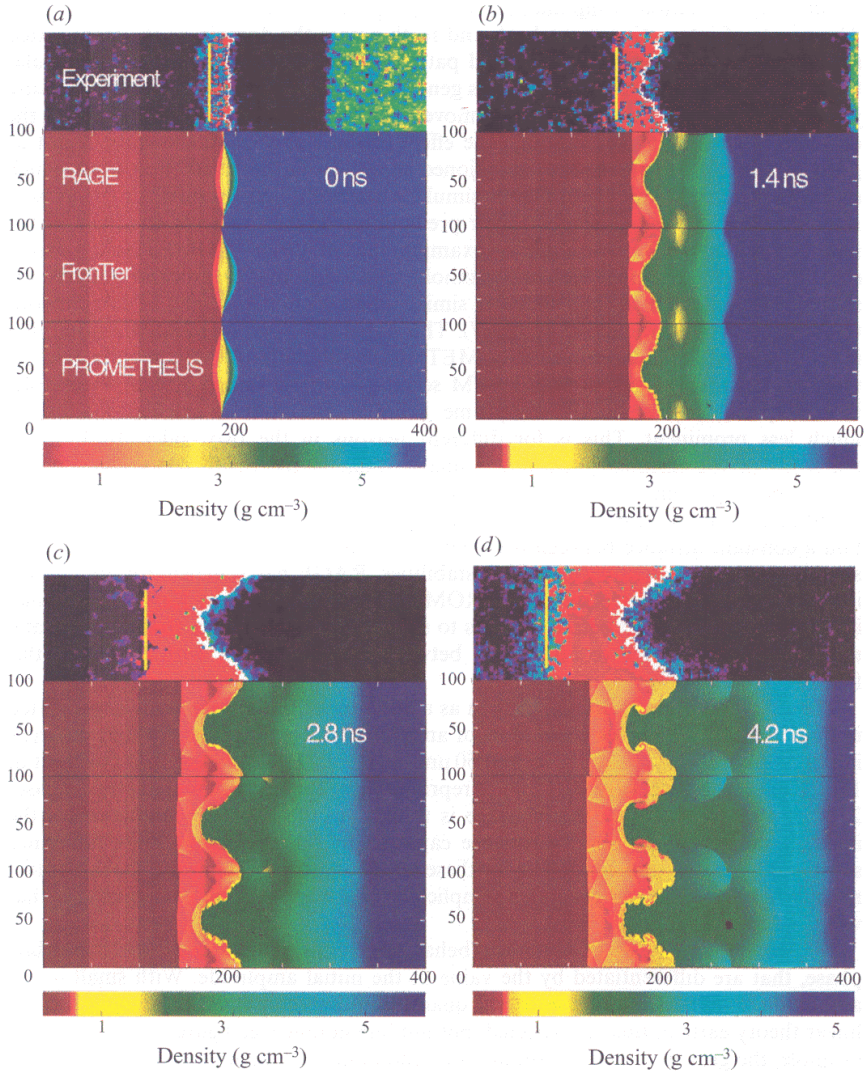

FIGURE 3. Simulation density plots and experimental radiographs for case 10/15.3. (*a*) $t = 0.0$ ns, (*b*) $t = 1.4$ ns, (*c*) $t = 2.8$ ns, (*d*) $t = 4.2$ ns. Each figure shows the results obtained with the three codes (RAGE, FronTier and PROMETHEUS, top-to-bottom) along with an experimental image. The incident shock moves from right to left. The experimental radiograph is an averaged composite over four wavelengths. Note that at later times the experimental wavelength increases due to expansion of the experimental target.

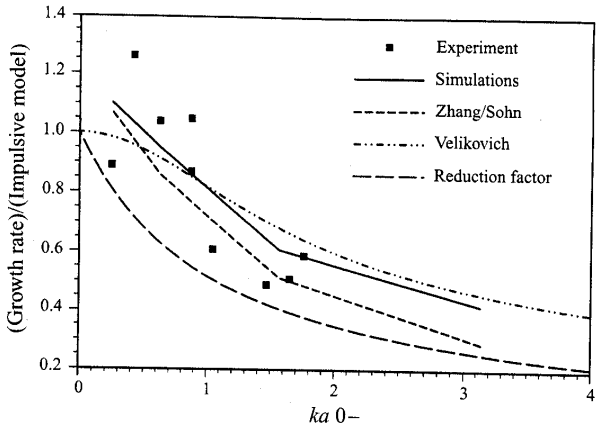

FIGURE 7. Comparison of experimental, simulation and theoretical peak growth rates as a function of initial amplitude with incident Mach number 15.3. Growth rates are scaled to the Meyer–Blewett formulation of the Impulsive Model. For the simulations we averaged the peak growth rates of each of the three codes.

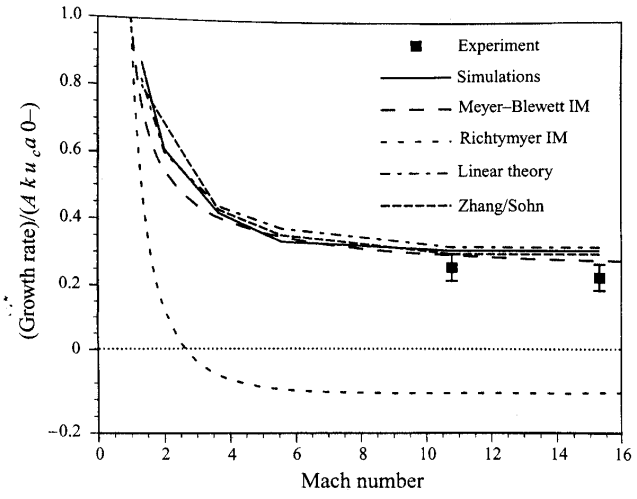

FIGURE 10. Comparison of experimental, simulation and theoretical peak growth rates as a function of incident shock Mach number. The growth rate is scaled by $Aku_c a_{0-}$.

Richtmyer-Meshkov: Late-time behaviour (Multimode)

Theory suggests $h \sim t^{\theta}$ for single shock RM

Nova experiment (Dimonte, Frerking, Schneider, PRL, vol 74, p4855 (1995)

Be/foam interface, random perturbations experiment gives $\theta \sim 0.6$.

2D CALE simulation with representation of the measured surface finish.

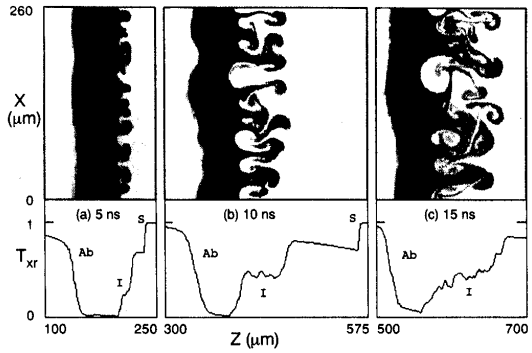

FIG. 4. Simulation side-on radiographs and spatial x-ray transmission profiles at $t = 0$, 5, and 10 ns.

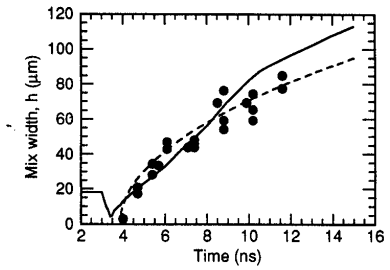

FIG. 5. The turbulent mix width at the interface vs time for the experiment (points), CALE (solid line), and Eq. (3) (dashed line) with $\eta_{\rm rms} \sim 4.6$ μm, $h^*_{0e} = 5.6$ μm, and $t_i = 3.9$ ns.

Mügler and Gauthier. Physics of Fluids, vol 12, p1783 (2000)

2D multimode RM mixing compare with shock tube experimental data.

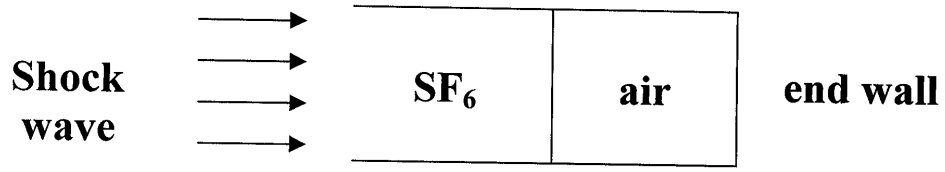

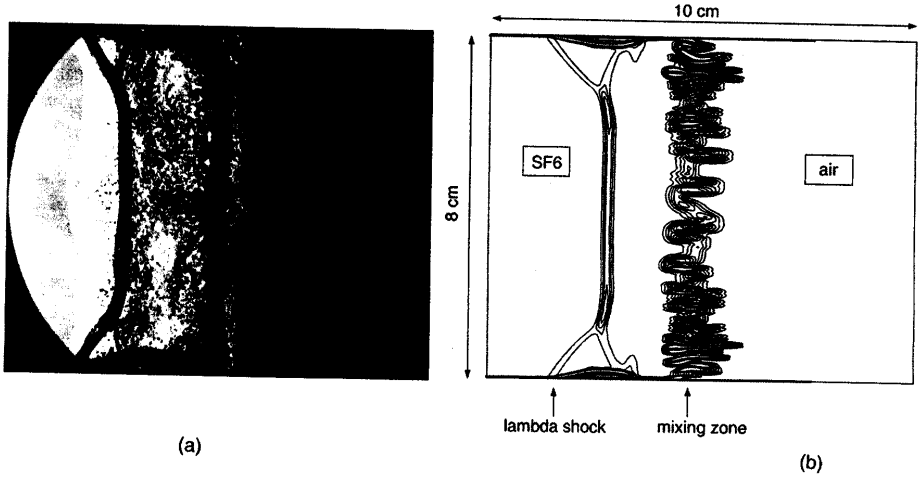

FIG. 7. (Color) (a) Experimental, from Galametz (Ref. 5), and (b) numerical schlieren pictures at a time t just after the first reflected shock wave–mixing zone interaction. Because of its interaction with the boundary layer, the transmitted shock in the SF_6 bifurcates.

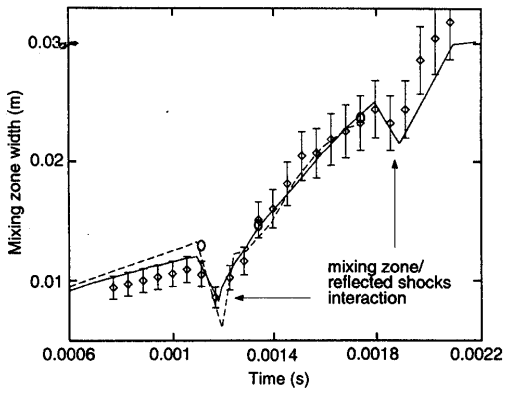

FIG. 2. Evolution of the mixing-zone width vs time. Diamonds correspond to the experimental width measured from schlieren pictures. The errorbars of this visual measurement are equal to ±10%. The three small circles correspond to microdensitometry measurements of some schlieren pictures. Full and dotted lines correspond to numerical widths obtained from the coarse and fine grids, respectively.

ADDITIONAL PHYSICS

Numerical simulation has played a major role in the understanding of additional physics on RT/RM instability.

(a) Material strength (solids)

(b) Density gradient stabilisation

(c) Ablation front stabilisation

Effect of Material Strength

Linear theory not straightforward.
Growth rate depends on
- **amplitude**
- **wavelength**
- **shear modulus**
- **yield strength**

Simplest model : amplitude threshold (Drucker)

Initial paper : J F Barnes et al J Appl Phys, vol 45, p727 (1974) **(LANL)**

Also : Swegle and Robinson. J Appl Phys, vol 66, p2838 (1989) **(SNLA)**

2D Lagrangian numerical simulation.

Swegle and Robinson

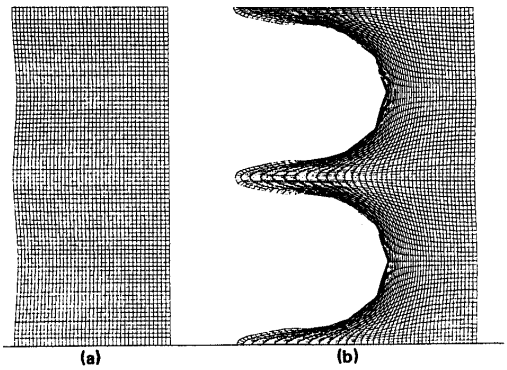

FIG. 2. Typical mesh plot for an unstable calculation. The small initial perturbation in (a) grows to that in (b) after a few microseconds of application of the driving pressure. There are 40 zones through the plate thickness of 2 mm, with 80 zones in the other direction.

Hydrodynamic Instability in Strong Media – UCRL – CR – 126710 (LLNL)

- Review of open VNIIEF publications

Theory, experiment, numerical simulation

2D (planar) vs 3D (axisymmetric)
2D grows faster than 3D (opposite to the fluid case)

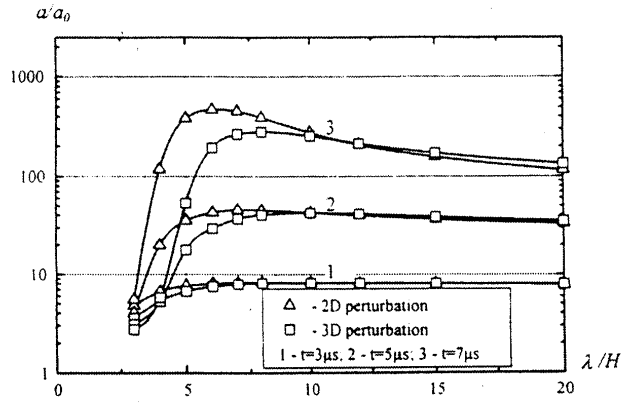

Fig. 4.3-14. Perturbation amplitude vs wavelength at various times for 2D and 3D perturbations. a_0=3.3 μm, σ_T=1.5 GPa, $\Delta\tau$=2 μs.

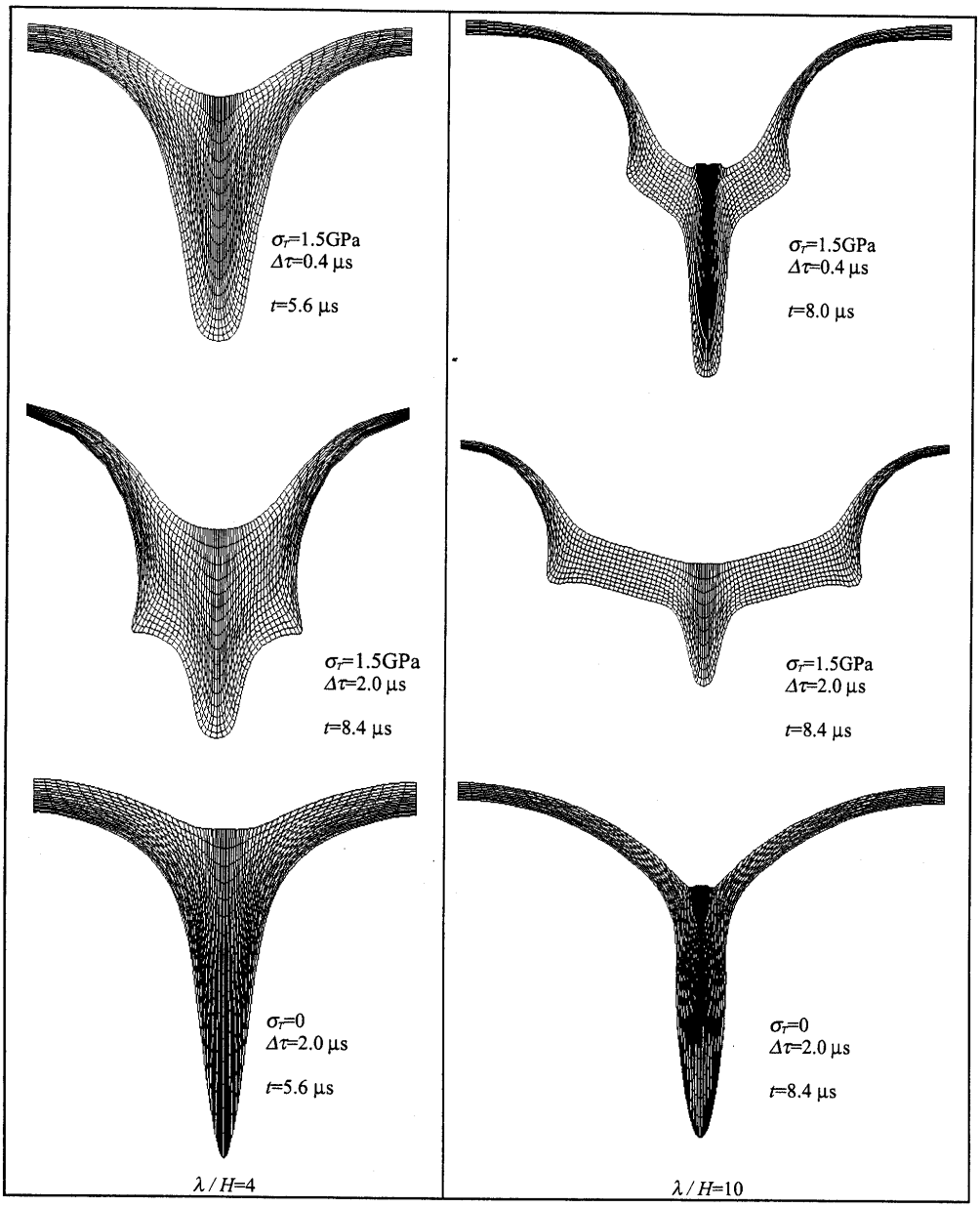

Fig. 4.3-13. Characteristic layer shapes.

Density gradient stabilisation

Pham and Meiron, Physics of Fluids, vol A5, p344 (1993)

RM + continuously stratified fluids
2D single mode and multimode.

Implusive acceleration

$$\rho(\mathbf{x},\mathbf{y})=\frac{\mathbf{1}}{\mathbf{2}}\left[\mathbf{1}+\mathbf{A}\tanh\left\{\frac{\mathbf{y}-\zeta(\mathbf{x})}{\mathbf{L}}\right\}\right]$$

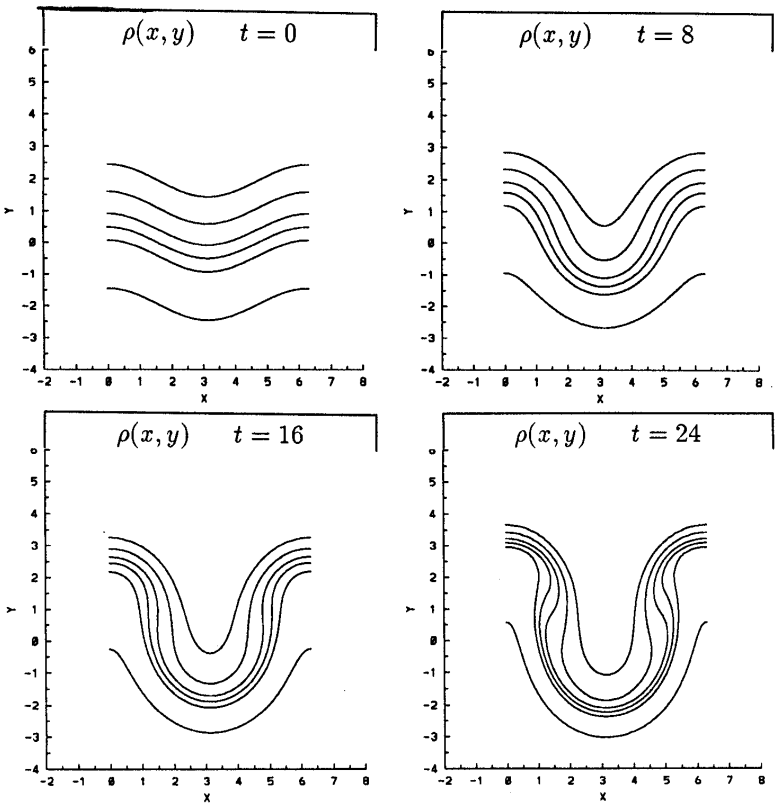

FIG. 1. Time evolution of the density contours for the single-scale profile $L=1.0$, $A=-0.5$, $\epsilon=0.5$, $t=0,8,16,24$. The contours are at $\rho=0.26,0.3,0.4,0.5,0.6,0.74$ in that order from top to bottom of each figure.

Ablative Rayleigh-Taylor instability

Ablation stabilisation is a key issue for direct-drive ICF as this reduces the growth of Rayleigh-Taylor instability.

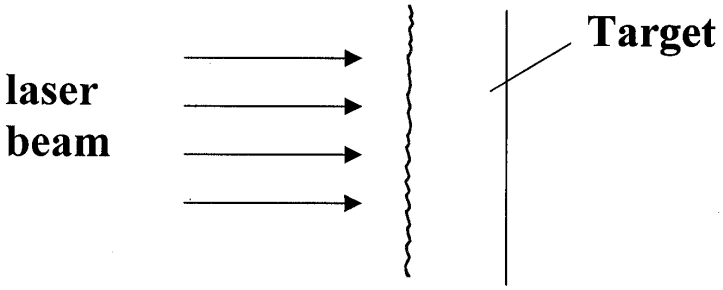

2D and 3D numerical simulations of ablative RT have been performed by the NRL group – also some of the first 3D RT calculations – Dahlburg and Gardner, Phys Rev A, vol 41, p5695 (1990) – mixing rate higher in 3D that 2D

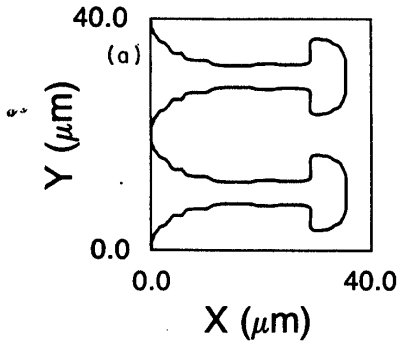

2D

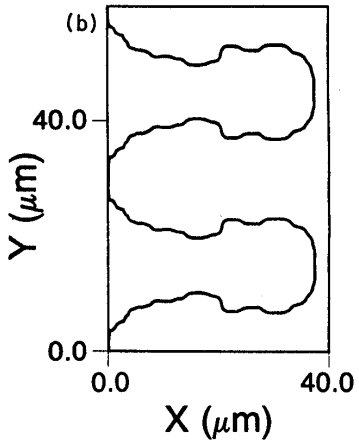

3D

3T Multimode ablative RT instability

Dahlburg et al, Phys Plasmas, vol 2, p2453 (1995)

FAST3D code – FCT method

220 x 128 x 128 cells

Random perturbation k^{-2} spectrum

In the case considered, ablative RT did not give fully developed turbulence.

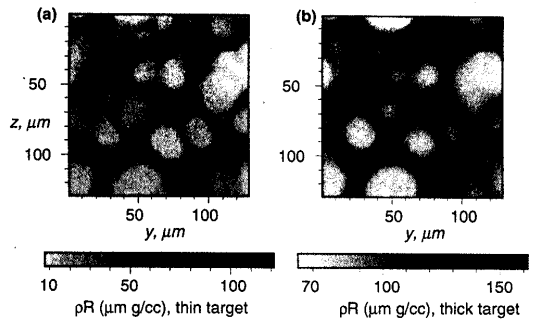

FIG. 4. Comparison of ρR between the thinner (a) and thicker (b) targets, at 4 ns when the thinner target has burned through. In these plots, the darkest shades of gray scale indicate the regions of greatest ρR.

3D SIMULATION

(a) Single mode/few modes

Difference between the behaviour of large scale structure in 2D and 3D.

3D growth rate is higher than 2D growth rate.

(Layzer theory).

Use of interface tracking is an advantage.

(b) Turbulent Mixing

Formation of a Kolmogorov-like $\left(k^{-\frac{5}{3}}\right)$ inertial range .

Dissipation in 3D much higher than in 2D. Counteracts the higher growth rate of the large scale structures in 3D.

Tryggvason and Unverdi Phys Fluids, vol A2, p656 (1990)

Single mode RT (2D vs 3D)
Boussinesq limit + viscosity
Accurate interface tracking method. Interface represented by triangular elements.

3D growth greater than 2D growth.

FIG. 2. The large-amplitude stage for a single initial mode. Here $t = 2.75$.

FIG. 1. The evolution of an interface disturbed by two modes. The nondimensional times are 2.0, 2.5, and 3.0.

RT Single Mode at Higher Atwood No.

Oparin and Abarzhi. Phys Fluids, vol 11, p3306 (1999) quasi-monotonic grid – characteristic method.

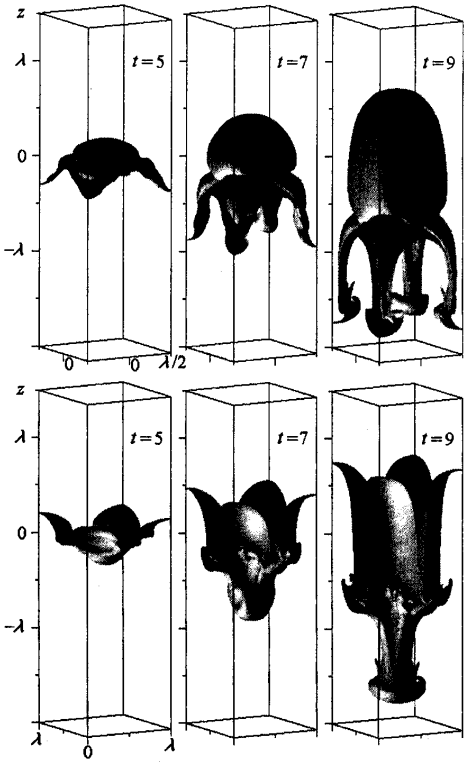

$\frac{\rho_1}{\rho_2} = 10$

FIG. 1. Bubble (above) and jet (below) evolution. Grid 30×30×210.

He, Zhang, Chen and Doolen. Physics of Fluids Vol 11, p1143 (1999) – Lattice Boltzmann scheme

Mixing of immiscible fluids.

$\frac{\rho_1}{\rho_2} = 3$

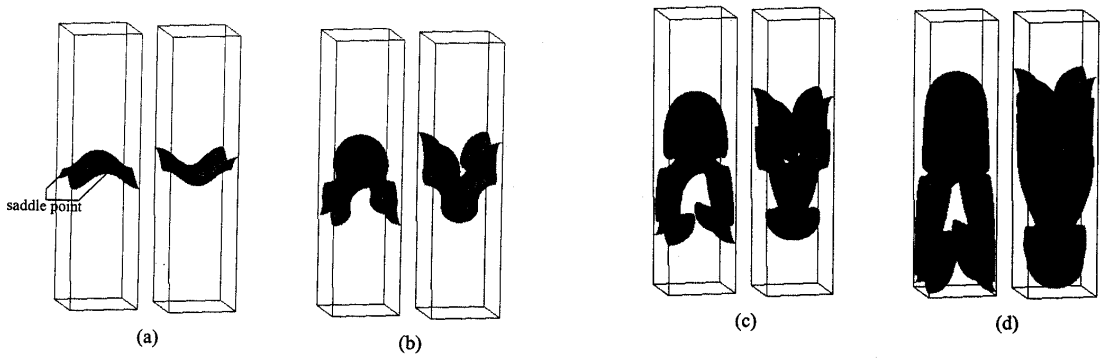

V.V.Nikishin et al. 6th IWPCTM (Marseille, 1997)

Institute for Mathematical Modelling
Lebedev Institute

3D single single mode/ few mode RM

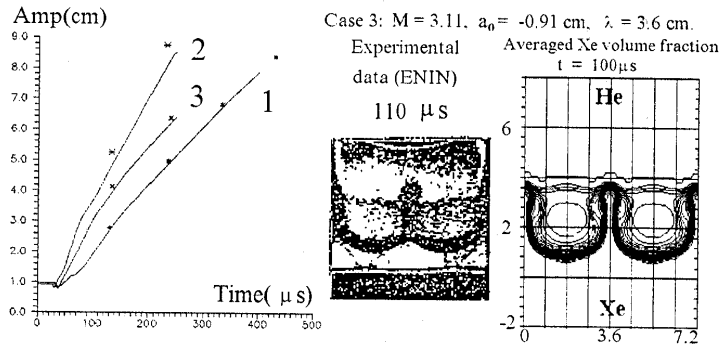

Figure 5. Comparison $He - Xe$ 3D results (ENIN,IMM,AWE).

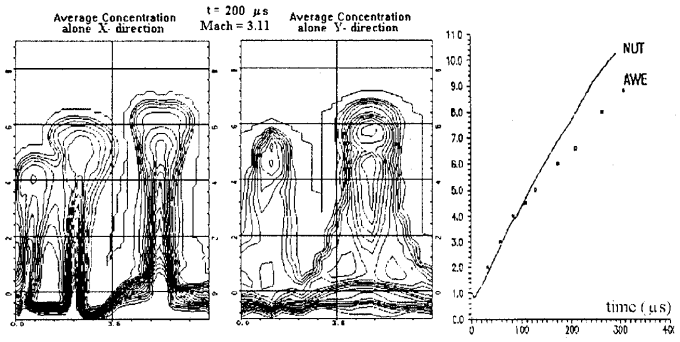

Figure 6. Multimode $He - Xe$ 3D results.

Li and Zhang. **Phys Fluids, vol 9, p3069 (1997)**

2D and 3D single mode
TVD method + Artificial Compression

Single shock : good agreement with non-linear theory of Zhang and Sohn.
3D growth > 2D growth.

Also single shock + reflected shock.

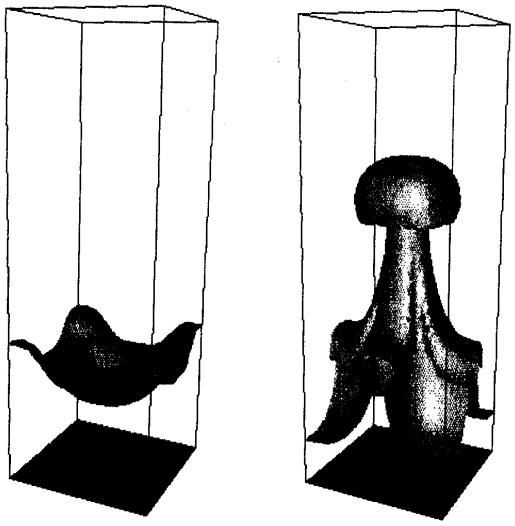

$t = 22.1$ $t = 58.6$

FIG. 10. Evolution of fluid interface in the Richtmyer-Meshkov re-shock experiment. The fluid interface first moves downward after transition of the incident shock. It is then hit by the reflected shock. Since the reflected shock travels from heavy fluid to light fluid, it is the reflected rarefaction case which reverses the phase of the interface motion. A mushroom-like spike is formed at $t = 58.6$.

SPHERICAL IMPLOSIONS (ICF)

Sakagami and Nishihara – PRL, vol 65, p432 (1990)

Town and Bell – PRL, vol 67, p1863 (1991)

(r, θ, ϕ) grid : $\frac{1}{120}$ of the sphere.

RT at inner fuel/shell interface.
Single mode spherical harmonic perturbation.

3D growth > 2D growth.

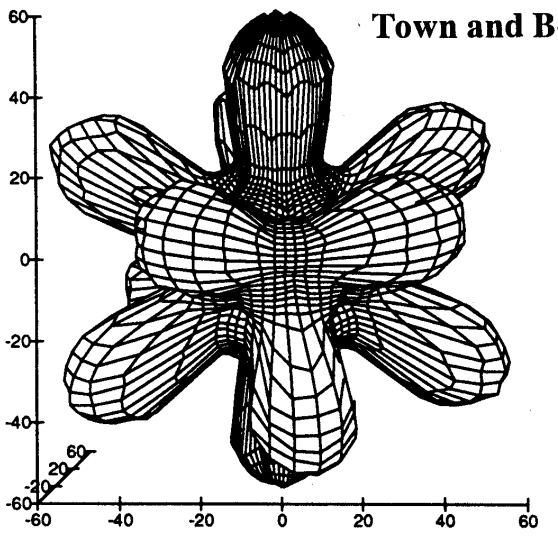

FIG. 1. The inner surface of the shell (defined as the surface of constant density equal to $1/e$ of the maximum density) at 1.226 ns. This shows the bubble-ridge arrangement.

Marinak et al, **Physics of Plasmas, vol 5, p1125 (1998)**

3D multimode RT calculations for NIF capsules.

(r, θ, ϕ) mesh
170 x 64 x 64 zones

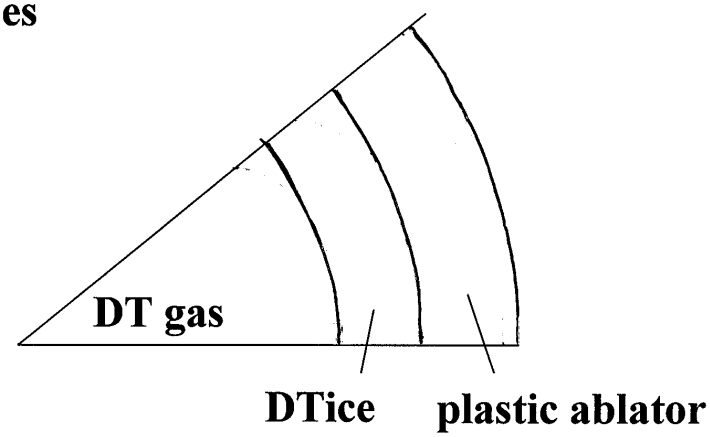

Realistic surface finish

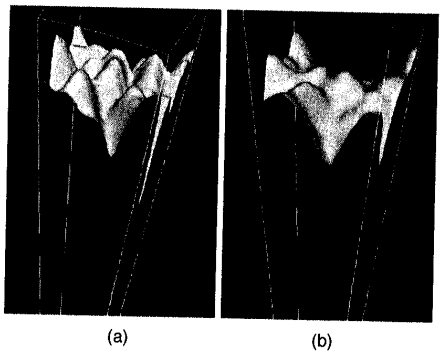

FIG. 9. Density isosurfaces close to the ablator–fuel interface 20 ps before the respective ignition time for each capsule. (a) For the PT capsule and (b) for the BeCu capsule.

3D TURBULENCE SIMULATION

Most detailed analysis for RT mixing – the simple case ρ_1, ρ_2, g constant – for which bubble growth is given by

$$h_1 = \alpha \frac{\rho_1 - \rho_2}{\rho_1 + \rho_2} gt^2$$

Major area of controversy is the treatment of the small scales

Techniques used

- **Direct Numerical Simulation (DNS) – viscosity and diffusivity included in the calculation – all scales present are resolved**
- **Interface tracking - for immiscible mixing**
- **Large Eddy Simulation (LES) - only large scales resolved - dissipation at small scales modelled**

The high-Reynolds number limit

In high-Reynolds number turbulent mixing, turbulence KE and density fluctuations are dissipated by a cascade to high wave numbers.

Power spectrum: $\sigma^2 = \int_0^\infty P(k)\, dk$

where $\sigma^2 = \left\langle \left(\mathbf{u}_i - \bar{\mathbf{u}}_i \right)^2 \right\rangle$ **or** $\left\langle (\rho - \bar{\rho})^2 \right\rangle$

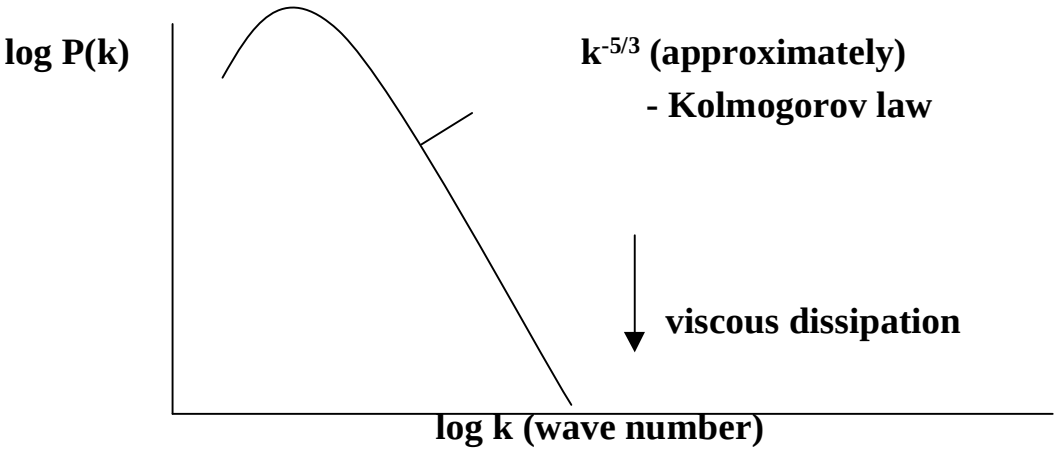

Viscosity/diffusivity determines the scale at which dissipation occurs, not the rate.

LES works if some of the $k^{-5/3}$ spectrum can be resolved – dissipation occurs at an artificially large scale determined by the mesh resolution.

(Conclusions given here are not necessarily applicable to simulation of turbulent boundary layers.

Experimental density fluctuation spectra

J Fluid Mech, vol 399, p1 (1999)

S. B. Dalziel, P. F. Linden and D. L. Youngs

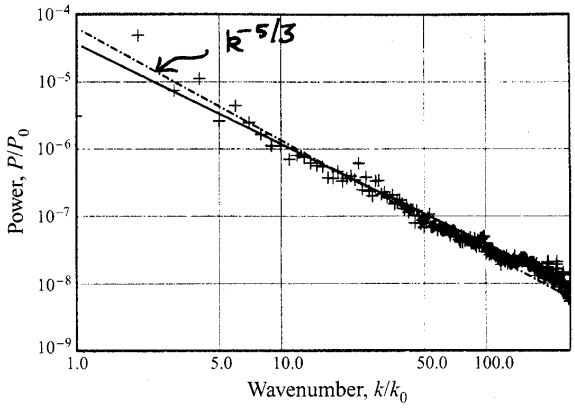

Sc=1000

Wilson and Andrews, Phys. Fluids, vol 14, p938 (2002)

Pr (Sc)=7

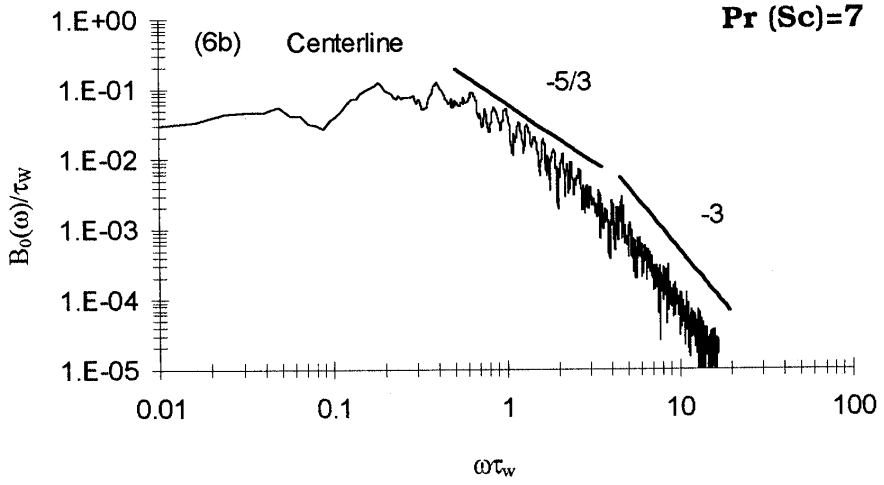

Two approaches to LES

See recent text books:-

Turbulent Flows: Stephen Pope, Cambridge University Press (2000)

Numerical Simulation of Reactive Flow (second edition) : Elaine Oran and Jay Boris, Cambridge University Press (2000)

(a) **The numerical method should have negligible dissipation.**
> 80% of the turbulence KE should be resolved
A sub-grid scale model should be used to represent the effect of the unresolved scales.

(b) **Many numerical schemes (FCT, van Leer, TVD) have implicit dissipation at high-wave numbers. No additional sub-grid model should be used.**
- **MILES, Monotone Integrated Large–Eddy Simulation**

(a) is most popular within the turbulence community – a controversial issue but not given much attention so far at the IWPCTMs.

Limited application of sub-grid models to RT/RM mixing.

LES + Smagorinsky model

Simplest and most well-known sub-grid model.

For incompressible uniform density flow

$$\frac{\partial u_i}{\partial t}+\frac{\partial}{\partial x_j}\left(u_i u_j\right)=-\frac{1}{\rho}\frac{\partial p}{\partial x_i}$$

$\bar{u}_i$ **= filtered value of** u_i **ie averaged over a small region of space just sufficient for** $\bar{u}i$ **to be resolved by the numerical mesh**

$$\frac{\partial \bar{u}_i}{\partial t}+\frac{\partial}{\partial x_j}\left(\bar{u}_i\,\bar{u}_j\right)=-\frac{1}{\rho}\frac{\partial \bar{p}}{\partial x_i}+\tau_{ij}$$

$$\tau_{ij}=\bar{u}_i\,\bar{u}_j-\overline{u_i u_j}$$

$$=2\nu_t\,\bar{S}_{ij}+\frac{1}{3}\tau_{kk}\delta_{ij}$$

$$\bar{S}_{ij}=\frac{1}{2}\left(\frac{\partial \bar{u}_i}{\partial x_j}+\frac{\partial \bar{u}_j}{\partial x_i}\right)$$

$$\nu_t=C_d\,\Delta x^2\left|\bar{S}\right| \qquad \text{where} \quad \bar{S}^2=\bar{S}_{ij}\,\bar{S}_{ij}$$

$\frac{1}{3}\tau_{kk}$ **add to** $\bar{p}$

Vremen et al J Fluid Mech, Vol 399, p357, (1997)

Six subgrid scale models applied to the free shear layer (32^3 grid).

Smagorinsky model with constant coefficient did not perform well – too dissipative in laminar regions.

Best results with dynamic eddy–viscosity model, Germano, J Fluid Mech, Vol 238, p325 (1992).

$$\tau_{ij} = c_d \Delta x^2 \left|\overline{S}\right| \overline{S}_{ij}$$

c_d: a variable coefficient estimated from the velocity field filtered at two different levels Δx and $2\Delta x$.

Subgrid Scale Models

Theoretical analysis available.

eg for Smagorinsky model (Fureby et al, Physics of Fluids, Vol 9, p1416, 1997) – assuming spectrum

$$\nu_t = \mathbf{c}_D \Delta^2 |\mathbf{S}|$$

$$\mathbf{C}_D = \frac{4}{\pi^2} \frac{1}{\left(3\,\mathbf{C}_K\right)^{3/2}} = 0.042$$

Δ = **filter width**

$\mathbf{C}_K$ = **Kolmogorov constant**

MILES technique

Theoretical analysis lacking, except for recent work by Margolin and Rider, ECCOMAS, Swansea, UK (2001).

Analysis of truncation terms in nonoscillatory finite volume schemes – relate to SGS models.

"It appears that the reluctance of the community in general to accept implicit turbulence modelling is more due to lack of justification of the approach rather than any failure of application."

DNS - low to moderate Reynolds no.

needed to understand the transition to Turbulence.

Understand the behaviour of the high – wave number end of the spectra.

Effect of Schmidt no.

LES or MILES

- used to model the high–Reynolds number limit – relevant to many applications eg shock tube experiments.

INTERFACE TRACKING

- useful to understand the effect of `surface tension for mixing of immiscible fluids (a number of RT experiments have used immiscible fluids).

Immiscible fluids with negligible surface tension should give fine–scale mixing which behaves like miscible

mixing, at high Reynolds number.

TURMOIL3D experience

Numerical method used based on the 2D Eulerian technique for multimaterial flow developed ~ 1980.

- **Lagrangian phase + rezone (advection) phase**
- **Interface tracking**
- **Monotonic advection method of van Leer used in rezone phase for all fluid variables.**

Van Leer method very successful at giving a robust method with low numerical diffusion.

Applied to a wide range of compressible flows with shocks and density discontinuities.

- **TURMOIL3D – same basic numerical method as the 2D code**
- **As simple as possible eg perfect gas EoS**
- **Interface tracking not used, as dissipation of density fluctuations at small scales expected**
- **Use of the van Leer method implied non- linear numerical dissipation at scales of order the mesh size**

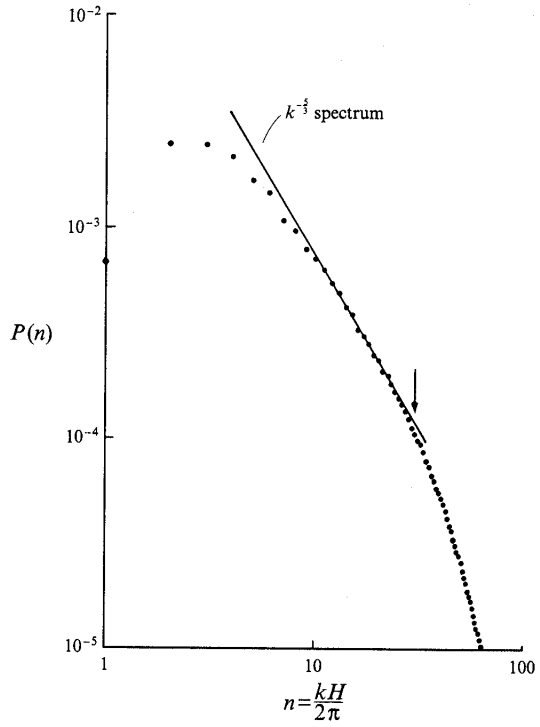

FIGURE 14. Power spectrum $P(n)$ for concentration fluctuations at $\tau = 3$ from the numerical calculation without the long-wave perturbation. The line drawn corresponds to a $k^{-\frac{5}{3}}$ spectrum, where $k = (k_x^2 + k_y^2)^{\frac{1}{2}}$. The arrow indicates the point where the wavelength $2\pi/k$ equals 6 mesh widths.

TURMOIL3D density fluctuation spectrum

Linden, Redondo, Youngs J Fluid Mech, vol 265, p97 (1994)

No need for additional sub-grid dissipation model

Could be argued that there is more high-wavenumber dissipation than desirable

MILES vs LES with explicit sub-grid model

TVD schemes (such as the van Leer advection method used in TURMOIL3D) have become very popular for compressible flow with shocks and contact discontinuities. It seems appropriate to continue using them for compressible turbulent flow. The dissipation implicit in the numerical scheme should be sufficient to make sub-grid models unnecessary $\rightarrow$ MILES approach.

The rationale for LES + explicit sub-grid model requires the use of a basic numerical technique with negligible dissipation $\Rightarrow$ TVD schemes cannot be used.

Does this mean that this approach is most useful for uniform density incompressible flow?

Many disagreements about best method to use for 3D RT turbulent mixing.

Need to compare results for agreed test problems.

Guy Dimonte (alpha group comparison).

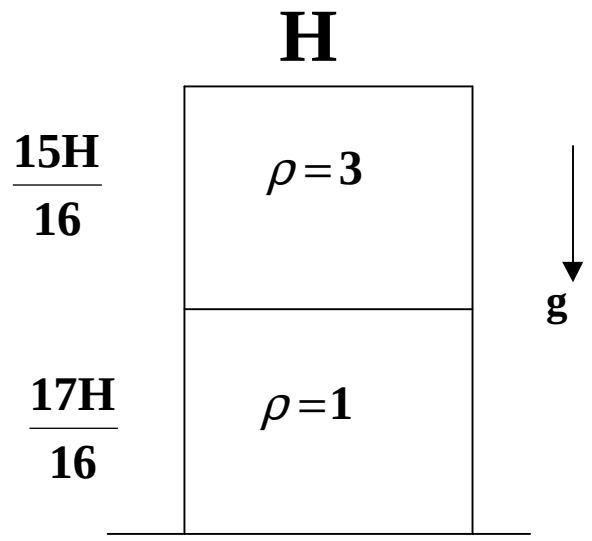

256 x 256 x 512 zones

Initial perturbation : wavelengths in the range 4 Δx to 8 Δx.

Growth by mode coupling $\Rightarrow$ loss of memory of the initial conditions.

$$h_1 = 3.3\int \overline{f_1} \cdot \overline{f_2}\, dz$$

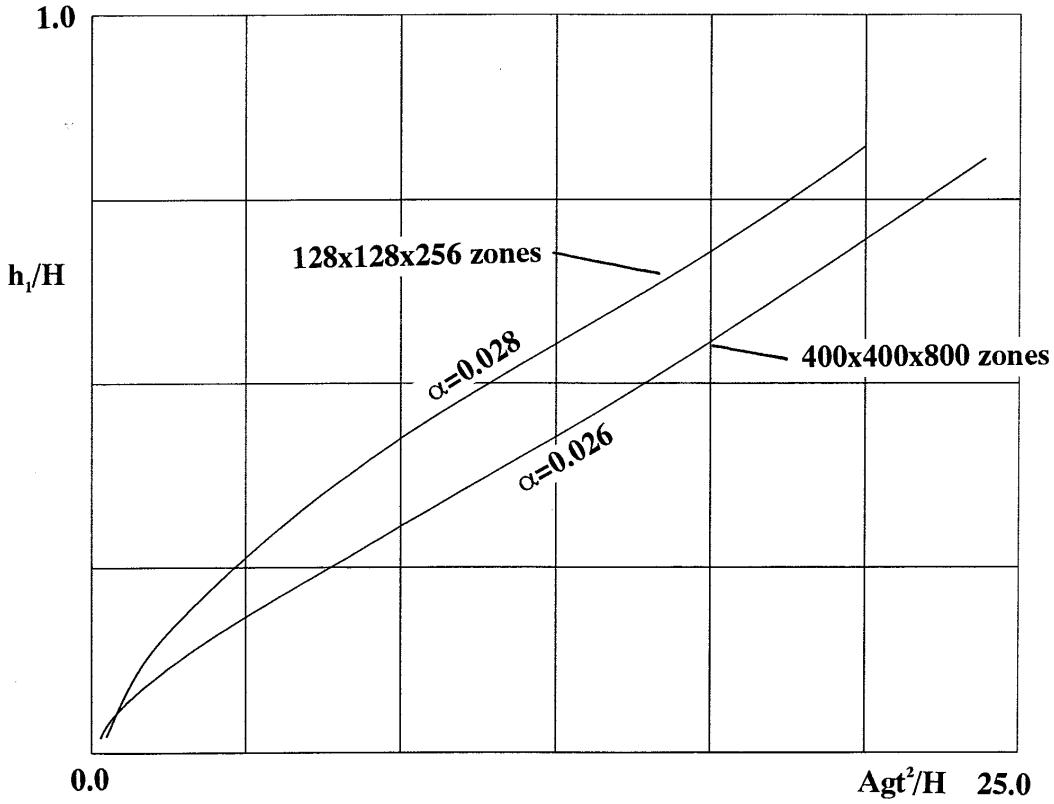

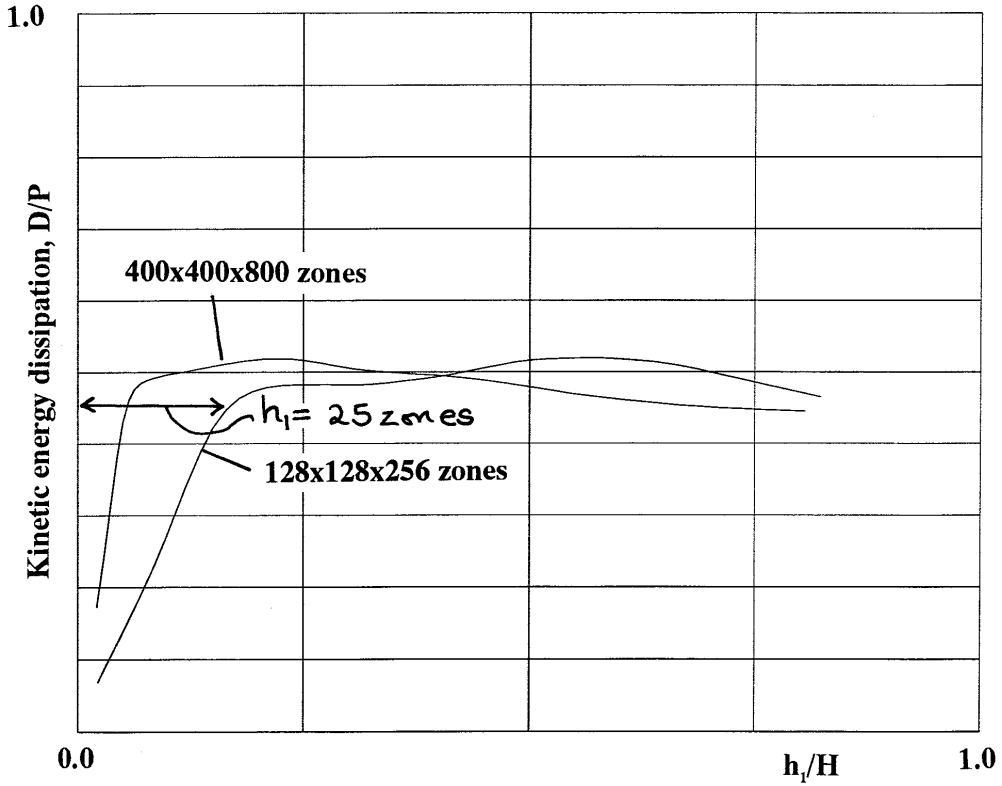
1.0
Kinetic energy dissipation, D/P
400x400x800 zones
h_1= 25 zones
128x128x256 zones
0.0
h_1/H
1.0

$$\theta = \frac{\int \overline{f_1 f_2}\, dz}{\int \overline{f_1}.\,\overline{f_2}\, dz}$$

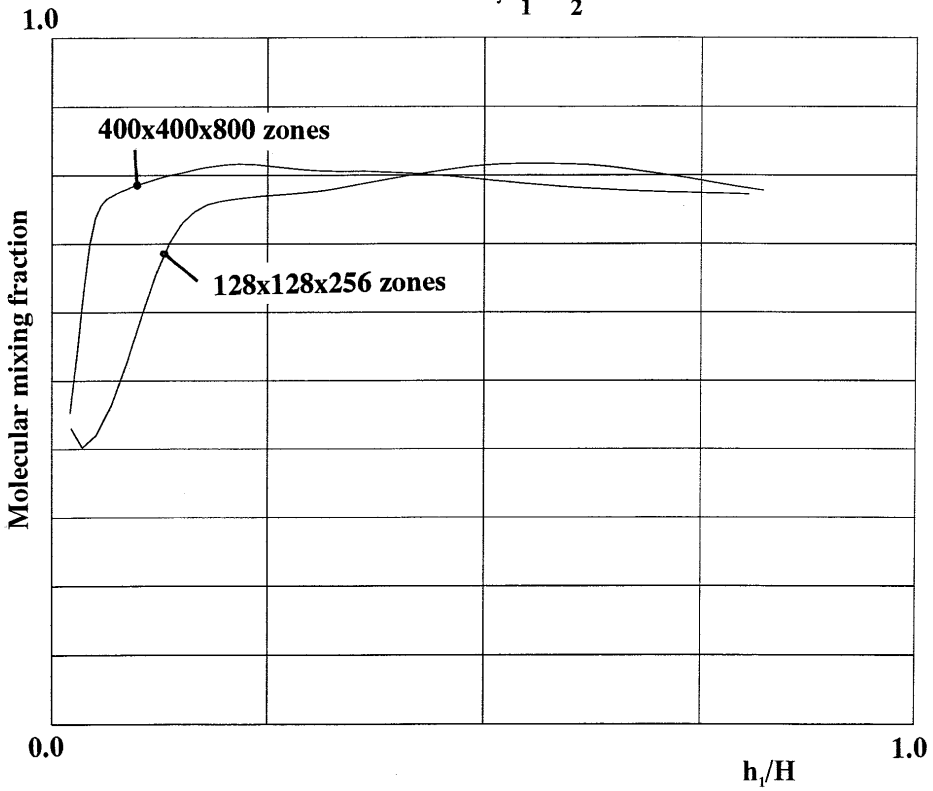

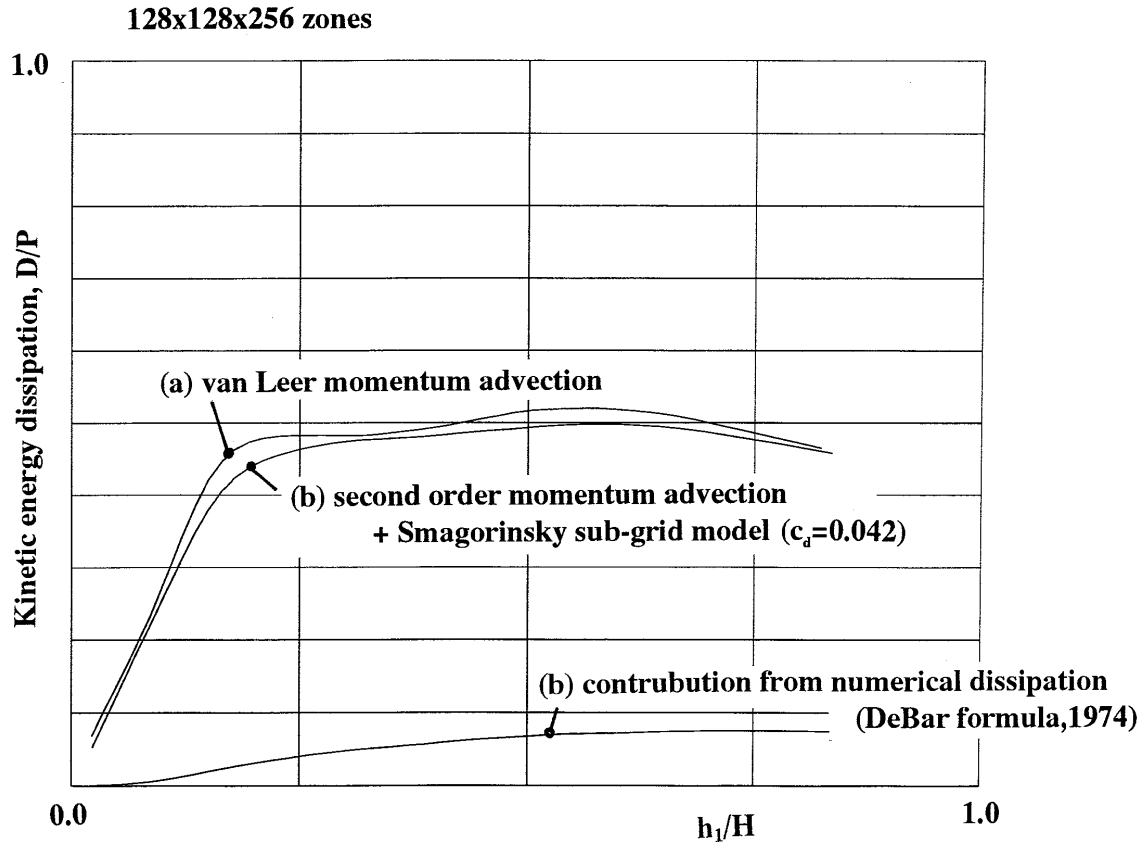
128x128x256 zones
1.0
Kinetic energy dissipation, D/P
(a) van Leer momentum advection
(b) second order momentum advection
+ Smagorinsky sub-grid model (c_d=0.042)
(b) contrubution from numerical dissipation
(DeBar formula,1974)
0.0
h_1/H
1.0

THE INITIAL PERTURBATION

RT experiments with constant g give bubble penetration

$$h_1 = \alpha \frac{\rho_1 - \rho_2}{\rho_1 + \rho_2} gt^2 \quad \text{, with } \alpha \sim 0.05 \text{ to } 0.06$$

TURMOIL3D calculations with short wavelength initial perturbations (growth purely by mode coupling) give

$\alpha \sim 0.03.$

Need to assume long wavelength initial perturbations with amplitude $\propto$ wavelength (as proposed by Inogamov) to give self-similar growth with $\alpha \sim 0.05$.

Perturbation used $\zeta(x,y) = \zeta_S + \zeta_L$

ζ_S **: wavelengths** $4\Delta x$ **to** $8\Delta x$

s.d $= 0.005\,\Delta x$

ζ_L **: power spectrum P(k)**

$$\sigma_\lambda = \left\{ \int_{2\pi/\lambda}^{\infty} P(k)\,dk \right\}^{\frac{1}{2}} = \varepsilon\,\lambda$$

$$\Rightarrow P(k) \propto 1/k^3 \text{ (ocean surface spectrum)}$$

$$\varepsilon = 0.0005$$

wavelengths in the range $4\Delta x$ **to** $\frac{H}{2}$

$\left(\text{ICF surface finish } P(k) \propto 1/k^2 \right)$

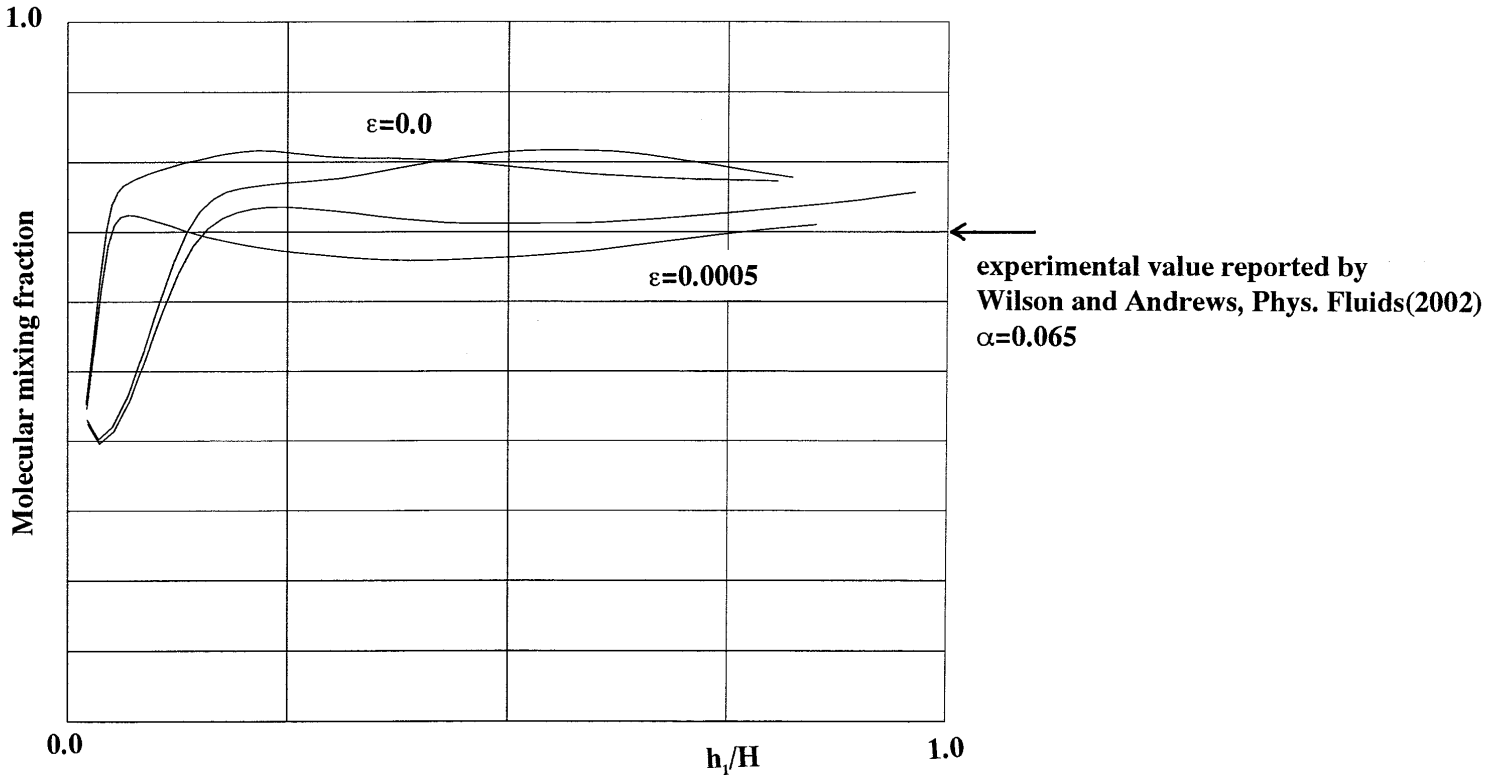
1.0
ε=0.0
ε=0.0005
Molecular mixing fraction
0.0
h1/H
1.0
experimental value reported by
Wilson and Andrews, Phys. Fluids(2002)
α=0.065

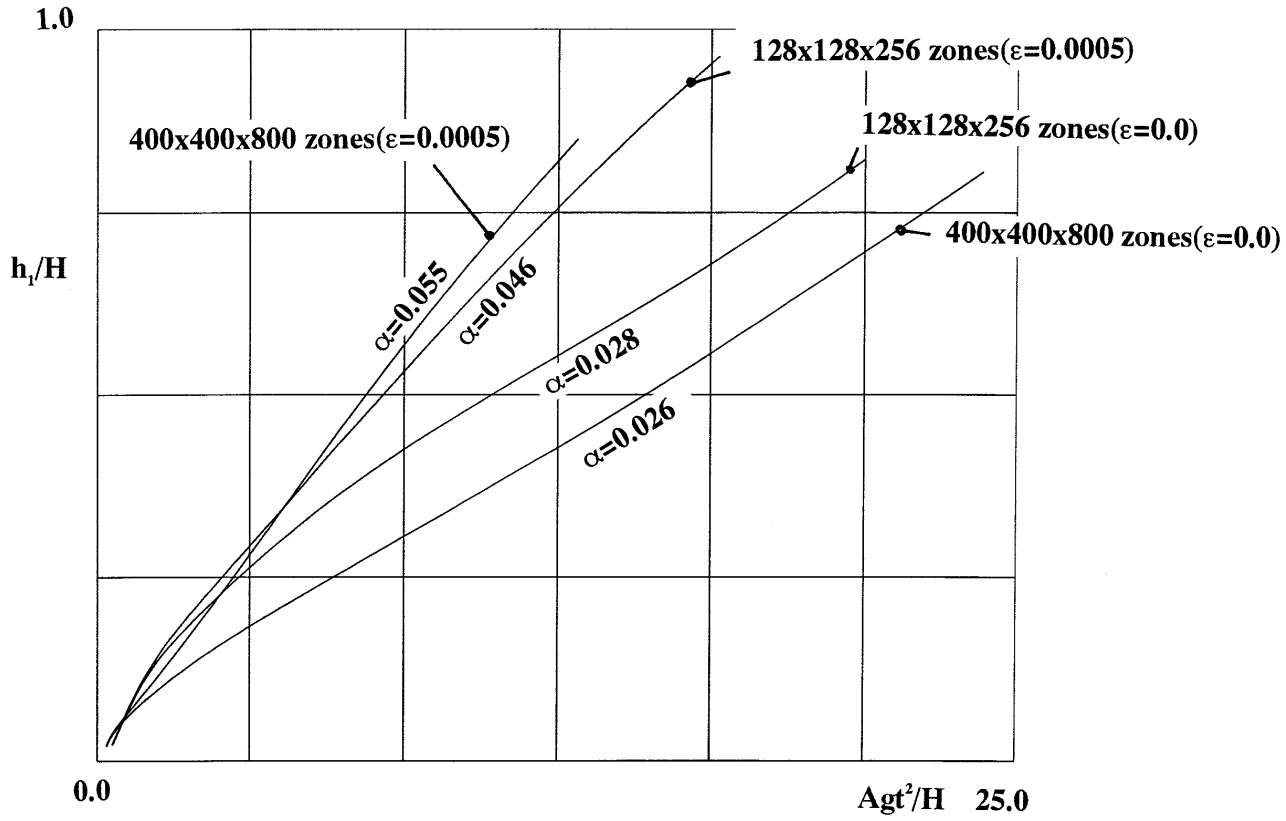
1.0
128x128x256 zones(ε=0.0005)
400x400x800 zones(ε=0.0005)
128x128x256 zones(ε=0.0)
400x400x800 zones(ε=0.0)
h1/H
α=0.055
α=0.046
α=0.028
α=0.026
0.0
Agt²/H 25.0

Figure7 : Probability distributions for f_1 within a plane z=constant

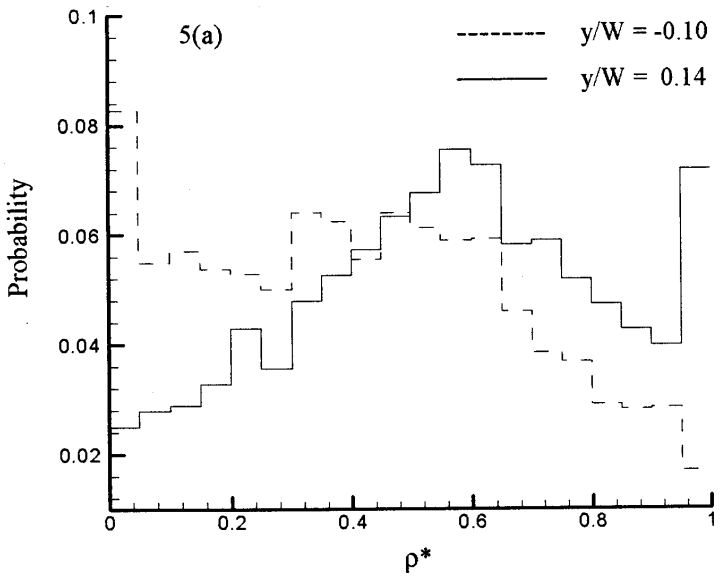

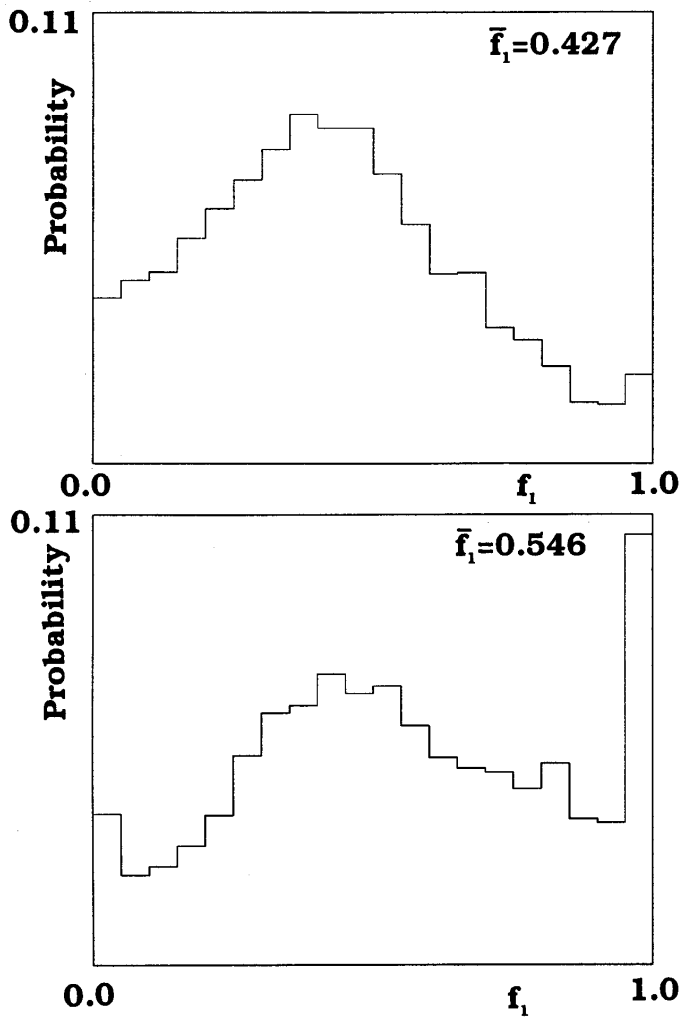

TURMOIL3D calculation
At=0.5
128x128x256 zones

g=constant

Cook and Dimotakis, J Fluid Mech, vol 443, p69 (2001)

DNS : 256 x 256 x 1024 zones

Sc = 1, Re ~ 140, $\rho_1/\rho_2 = 3$

Diffuse initial interface

Eighth-order compact scheme (Lele 1992) – spectral-like resolution.

Calculated transition to turbulence, which was found to be very dependent on the initial conditions.

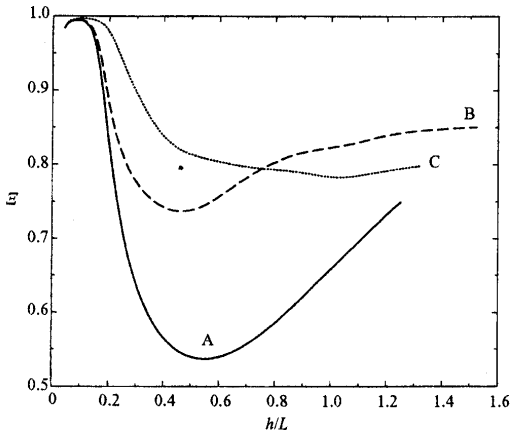

FIGURE 16. Mixing parameter, Ξ, *vs.* h/L, for the three cases.

Young, Tufo, Dubey, Rosner (Chicago U) – J Fluid Mech, vol 447, p377 (2001)

Miscible RT

Spectral method or spectral-element method
Low Atwood no. (Boussinesq approximation)
256 x 256 x 512 zones.
Initial modes with wavelengths around 8Δx.

2D $\alpha \sim 0.017$?

3D $\alpha \sim 0.03$

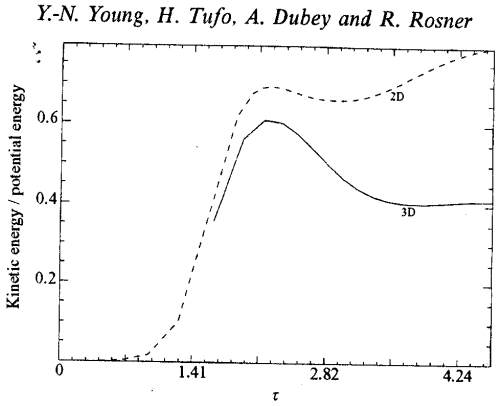

FIGURE 8. Ratio of kinetic energy to gravitational potential energy: two-dimensional versus three-dimensional simulations. The kinetic energy is the volume integral of the kinetic energy density, and the potential energy is the volume integral of the potential energy available in the system. For $\tau \leqslant 1.4$, the growth is exponential and is similar for both two and three dimensions, after this period, two-dimensional motions are much more efficient in extracting potential energy than three-dimensional motions.

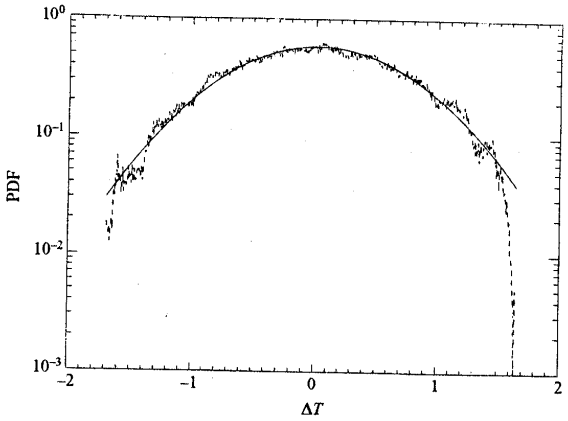

FIGURE 13. PDF of the temperature fluctuation ($\delta T = T - T_0$) within the mixing zone ($\Delta z = 0.025$) at the position of the original interface ($z = 0.06$).

Calculations with Interface Tracking

A number of researchers have considered turbulent mixing of immiscible fluids using interface tracking techniques.

J Glimm et al J Comp Phys, Vol 162, p652 (2001)

Frontier method – represents both the velocity and density discontinuity at the interface.

112 x 112 x 224 zones

α ~ 0.07

Oron, Arazi, Kartoon, Rikanati, Alon, Shvarts Physics of Plasmas, Vol 8, p2883 (2001). See also Shvarts et al Shock-Induced instability of interfaces, in Handbook of Shock Waves, Vol 2, Academic Press (2001).

80 x 80 x 80 zones

α ~ 0.05

Anuchina et al – Proceeding of 5th Zababakhin Scientific Talks (1999).

60 x 60 x 60 zones **α = 0.064**

120 x 120 x 120 zones **α = 0.074**

Evidence for $k^{-5/3}$ energy spectrum.

(Also, Yu. V. Yanilkin, VNIIEF, 120^3 mesh, α = 0.06)

Rayleigh-Taylor Summary

- **Many 3D calculations with significant differences between results**

  α ~ 0.03 to 0.07

- **Effect of initial conditions important – very good reason for pursuing the numerical simulation.**

- **Controversy over the numerical techniques which should be used.**

  Use of sub-grid scale models is recommended by many but has not been widely used here.

  Interface tracking calculations have given higher values of α but have not used the highest resolution.

- **Need some test problems to resolve the disagreements (see talk by Guy Dimonte).**

RM Turbulent Mixing

Fewer 3D simulations available.

Scaling laws for single shock RM :

Bubbles	**:**	$h_B \sim t^{\theta B}$
Spikes	**:**	$h_S \sim t^{\theta S}$

Youngs, Laser and Particle Beams, Vol 12, p725, (1994)

160 x 160 x 270 zones, assumed $\theta_B = \theta_S$

then $\theta \simeq 0.30$ **(based on growth of integral mix width)**

for a flat spectrum

P(k) = const for 0 < k < k_{max}

$k_{max} = \dfrac{2\pi}{\lambda_{min}}$, $\lambda_{min} = 16\Delta x$

Cohen et al. IWPCTM6 (Marseille)

High resolution RM calculations up to 512^3

PPM method

Single-shock and double shock calculations

Single – shock random perturbations, but with longer wavelengths present

θ = 0.75

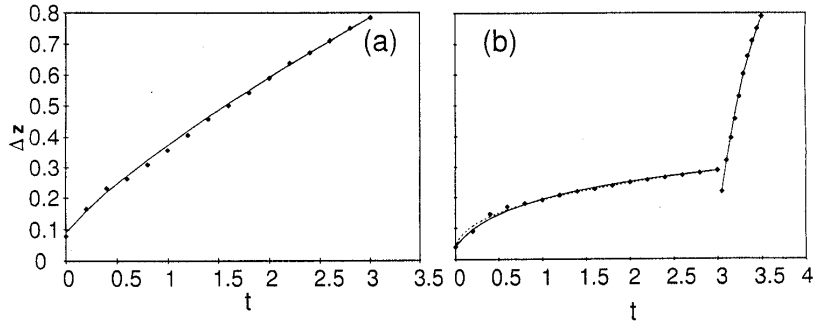

Figure 1. Mixing layer growth vs. time for (a) random-phase sum initial condition; (b) single mode initial condition with two shocks

Oron, Arazi, Kartoon, Rikanati, Alon, Shvarts

Physics of Plasmas, vol 8, p2883 (2001)

LEEOR-3D (interface tracking)

80 x 80 x 80 zones

$\theta_B \simeq 0.35\,(2D) \quad , \quad \sim 0.22\,(3D)$

$\theta_S \simeq 0.45\,(2D) \quad , \quad \sim 0.3\,(3D)$

Results used to construct a simple buoyancy – drag model.

Theta bubble:

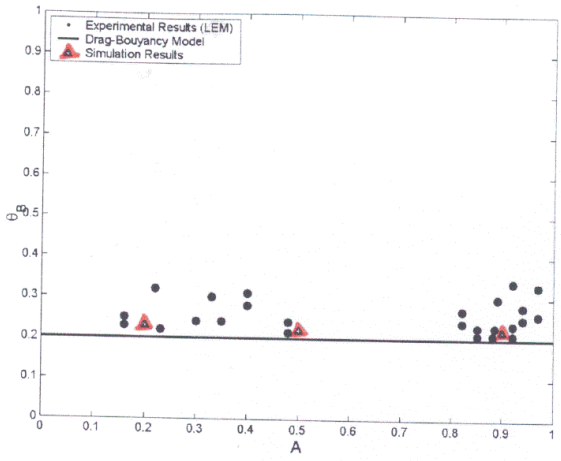

Theta spike:

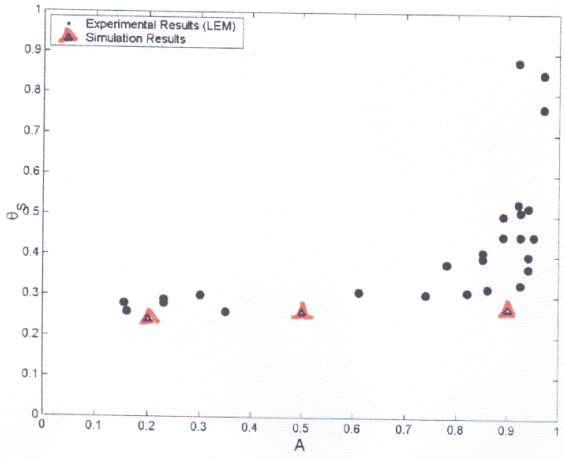

Single Shock RM

3D simulation should be used to investigate the effect of initial conditions in more detail.

An initial amplitude spectrum

$$P(k) \sim k^{-2}$$

may be more appropriate to real applications $\Rightarrow$ higher values of θ_S , θ_B ?

Double Shock RM

3D simulation has been applied to experiments where several shocks are present.

However, no detailed 3D studies (development of scaling laws) for double shock RM.

Second shock : shock-turbulence interaction and shock-density fluctuation interaction.

FUTURE ROLE OF NUMERICAL SIMULATION

2D Simulation

- **Will continue to be essential for complex problems with additional physics**

3D Simulation

- **Fundamental understanding of turbulent mixing in simple flows (DNS and LES)**
- **More complex flows – LES now feasible**
- **LES results should be used to validate engineering models (Bouyancy – drag models, RANS models)**
- **Not yet feasible for complex real applications**

AWE SHOCK TUBE EXPERIMENT

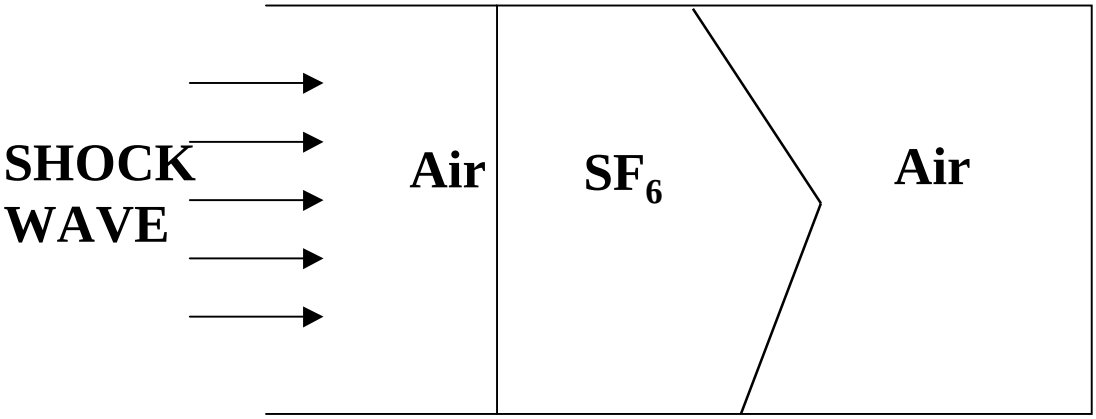

The purpose of the shock tube experiment is validation of a 2D RANS model

Experiment is 2D on average

3D Simulation (TURMOIL3D) : 400 x 320 x 160 zones interfaces randomly perturbed

2D turbulence model (RANS model) calculation

: 200 x 160 zones

Compare average behaviour extracted from 3D simulation with 2D RANS model

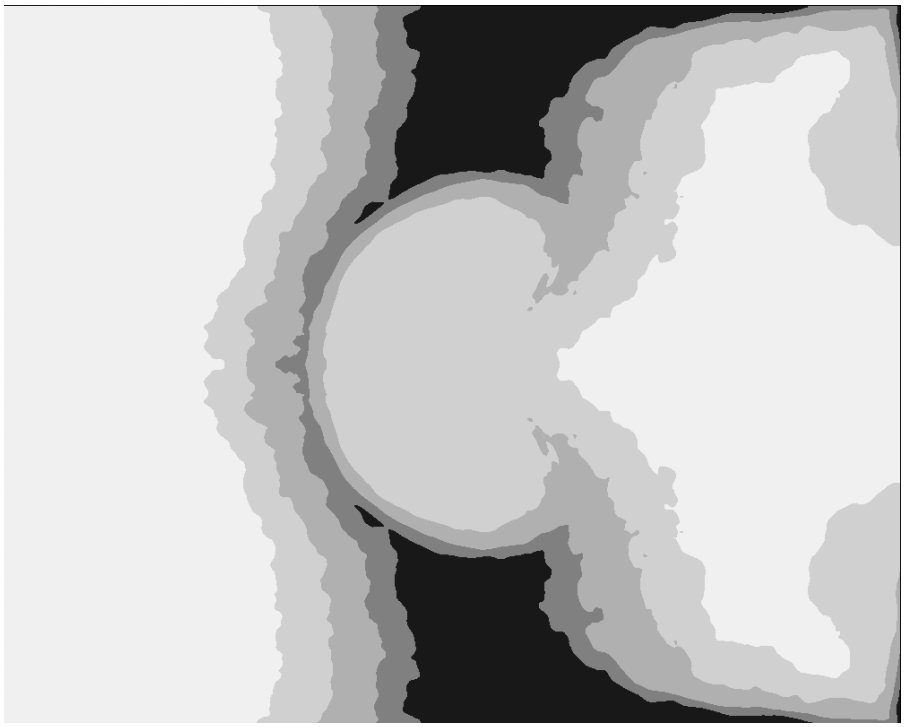

3D simulation at t = 4.0ms

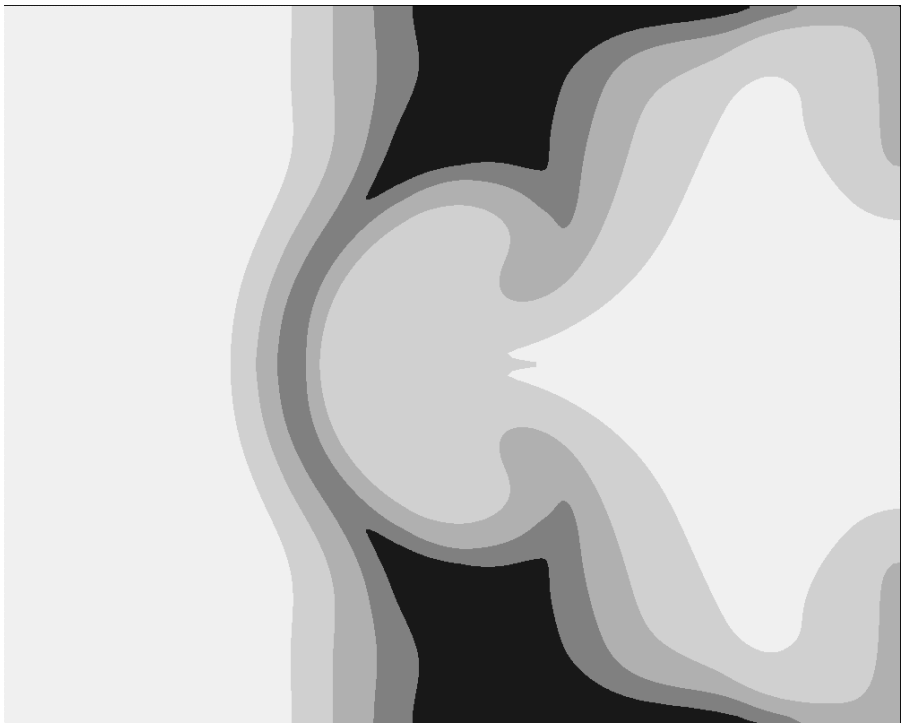

2D RANS model at t = 4.0ms

Mean volume fraction levels -

0.0,0.05,0.3,0.7,0.95,1.0

FINAL REMARKS

- **Numerical simulation has made a major contribution to the understanding of RT and RM instability over the last 40 years.**

- **Need to focus more now on 3D turbulence simulation.**

- **Reasonably good 3D LES can be performed with mesh sizes ~ 256^3, well within the capability of present-day supercomputers.**

- **3D simulation not yet practical for complex real applications but can have a major impact on engineering models.**